Using Electronic Circuits to Model Simple Neuroelectric Interactions

EDWIN R. LEWIS, MEMBER, IEEE

Abstract—**The Hodgkin-Huxley description of electrically excitable conductances is combined with the Eccles description of synaptic conductances to provide the basis of an electronic model of nerve-cell membrane. The models are used to explore neuroelectric interactions between spatially distributed regions of a single neuron and neuroelectric activities in very small groups of neurons. Among other things, oscillations are found to conduct with progressively increasing phase lead along an axon model. Miniature reflected spikes from a trigger region are able to reset slow potentials in an integrative region. Spike synchrony is found to be common in a mutually inhibiting pair of neural models. Spike bursts occur in a mutually exciting pair. Electrical connection between trigger regions is found to be excitatory or inhibitory, depending on phase relations.**

A simpler electronic model is described and shown to be reasonably adequate for simulation of small neural nets.

I. Introduction

USING A TECHNIQUE devised by Cole,[1] Hodgkin and Huxley[2]–[4] in 1951 applied voltage steps across isolated patches of squid-axon membrane and observed the time course of the current in each case. They resolved the current into a capacitive component and three ionic components (potassium-ion current, sodium-ion current, and leakage current due to all other ions). Defining the driving force for each of the three ionic currents as the difference between the actual voltage across the membrane and the voltage at which that particular current reversed, Hodgkin and Huxley described their results in terms of the equivalent circuit on the right of the dashed line in Fig. 1. Their experiments indicated that the equilibrium potentials V_K, V_{Na}, and V_L, the capacitance C_M, and the leakage conductance G_L were constant but that the equivalent potassium conductance G_K and the sodium conductance G_{Na} were functions of membrane potential and time. From their data, they were able to formulate explicit descriptions of G_K and G_{Na} which were valid within the constraints of their experiments (i.e., valid for stepwise changes of membrane potential). Then they set out to determine whether or not these descriptions, coupled with the equations for the equivalent circuit, could predict the responses of the unconstrained axon membrane. They could.

Manuscript received October 2, 1967. The research reported in this paper was sponsored by the Librascope Group, General Precision Systems, Inc., Glendale, Calif., under U. S. Air Force Office of Scientific Research Contract AF49(638)-1232; the 6570th Aerospace Medical Research Laboratories, Air Force Systems Command, under Contract AF33(615)-2464; and the Joint Services Electronics Program, under Grant AF-AFOSR-139-67.

The author is with the Department of Electrical Engineering and Computer Sciences and the Electronics Research Laboratory, University of California, Berkeley, Calif.

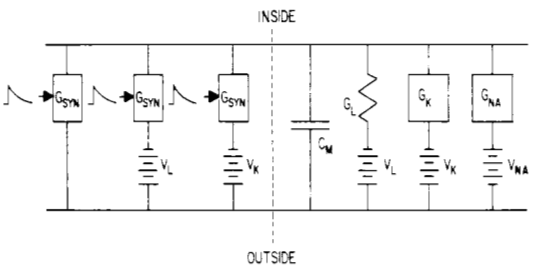

Fig. 1. A circuit representation of a patch of electrically excitable membrane contiguous with a patch of subsynaptic membrane. The horizontal conductor on the top of the circuit represents the conductive medium inside the nerve cell; the bottom conductor represents the conductive medium outside the cell. The four elements on the right of the dashed line are the four shunt admittances across an electrically excitable membrane according to the Hodgkin-Huxley description. The three elements on the left are the three shunt conductances across synaptic membrane according to the descriptions of Eccles.

In fact, they predicted virtually every aspect of the squid-axon spike in minute detail.[5] Hodgkin and Huxley's equivalent circuit, along with their descriptions of the time and voltage dependencies of the potassium and sodium conductances, thus provides an excellent model of spike generation in the squid axon and an excellent basis for models of spike generation in other axons.

By the mid 1950's, Eccles and others had found convincing evidence that many neurons communicate with one another chemically, not electrically.[6] Once again the data have been interpreted in terms of an equivalent electrical circuit (shown to the left of the dashed line in Fig. 1). Eccles inferred from the data that in response to a spike along its axon the sending cell emits a chemical transmitter substance. A component of conductance (the synaptic conductance) of the receiving cell membrane is directly proportional to the concentration of that transmitter substance in the space between the cells. The transmitter substance is inactivated, probably by a first-order process; so the synaptic conductance in the receiving cell rises rapidly during a spike in the sending cell and then falls exponentially toward zero. As Hodgkin and Huxley had done, Eccles and his coworkers found equilibrium potentials associated with the conductances of their circuit. Excitatory synaptic currents reversed when the membrane potential was close to zero, so the excitatory synaptic conductance in the equivalent circuit has no battery in series with it. The inhibitory synaptic currents reversed either at the potassium equilibrium potential, at the equilibrium potential for leakage current, or at some potential between the two. Two equivalent syn-

aptic conductances can account for all three types of inhibitory synaptic current. All three equivalent synaptic conductances were found to be independent of membrane potential.

By the late 1950's, microelectrode techniques had been improved, and Bullock and others began to observe some of the fine detail of neuroelectric potentials. In addition to spikes and potential fluctuations due to synaptic currents, they occasionally found spontaneous oscillations of the membrane potential.[7]–[10] Bullock called these oscillations "pacemaker" potentials and identified three types: sinusoidal, saw-toothed, and full periodic spikes. In addition, several complications were observed in the synaptic responses. Bullock[10] in fact specified three degrees of freedom for synaptically induced potentials: 1) A synaptic potential may be excitatory or inhibitory. 2) The amplitude of synaptic potentials may be enhanced, diminished, or completely unaffected by previous synaptic activity. 3) A burst of synaptic activity may result in residual excitation, residual inhibition, neither, or both (i.e., oscillations from one to the other). Finally, Bullock,[10] Eccles,[6] and others found that synaptic regions and pacemaking regions of nerve cells often exhibited completely graded activity rather than threshold effects and were incapable of conducting a spike.

One might reasonably ask whether or not the nerve-cell membrane in synaptic and pacemaker regions really is much different from the spike-conducting membrane of the axon. Will a combination of the synaptic model proposed by Eccles and a reasonable modification of the Hodgkin-Huxley model account for the potentials observed by Bullock and others? The answer, for the most part, is yes.

Electronic circuits were designed to simulate faithfully the seven elements of the combined system of Fig. 1. The capacitance C_M and leakage conductance G_L of course were very easy to simulate. Simulation of the potassium and sodium conductances, on the other hand, required elaborate nonlinear, active filters to transform the simulated membrane potential into the time- and voltage-dependent conductance functions specified by Hodgkin and Huxley. The decaying exponential, synaptic-conductance functions were simulated by simple RC filters. Since the current through a conductance is proportional to the product of the conductance itself and the voltage across it, the simulated conductance functions were transformed into equivalent conductances by means of electronic multipliers. The complete electronic model basically was a two-terminal network, with one terminal representing the conducting medium inside the nerve cell and the other terminal representing the conducting medium outside the cell. Between the terminals were seven circuits connected in parallel. The model was a point model in that it represented a patch of membrane over which there was no variation of potential. It may be considered to represent a patch of subsynaptic membrane with a contiguous patch of spike-generating membrane, or it may be considered to represent either a mosaic or a homogeneous mixture of the two. Since the circuit elements are parallel, these configurations electrically are equivalent.

With the parameters of the elements on the right side of Fig. 1 set to the values specified by Hodgkin and Huxley, the synaptic responses of the electronic model were examined. Each synaptic conductance had two parameters: the magnitude of the conductance increment per presynaptic spike, and the time constant of conductance decline. These parameters in conjunction with the three synaptic conductances proved to be completely sufficient to account for all of the synaptic degrees of freedom described by Bullock. Again with the parameters of the Hodgkin-Huxley elements set to their specified values, the electronic model was examined for oscillations. Oscillations could be induced in the model by any of several means,[11] including the application of dc current across the two terminals. When this current was small, nearly sinusoidal oscillations appeared; when the current was larger, saw-toothed oscillations appeared; when it was still larger, periodic spikes appeared. The model thus produced all of the types of the pacemaker potentials identified by Bullock. Finally, several parameters of the Hodgkin-Huxley model were found to affect its spike-generating ability. Many nonspiking regions of neurons, however, have been found to exhibit membrane capacitances considerably higher than those measured by Hodgkin and Huxley in the squid axon.[12]–[14] Increasing C_M to these values was sufficient to induce completely graded response in the model. Thus, with very minor parameter variations, the electronic realization of the combined Eccles-Hodgkin-Huxley models provided all the neuroelectric phenomena described by Bullock. The quantitive details of these results have been published elsewhere.[11],[15],[16]

In addition to producing all the potentials observed by Bullock, the electronic model predicted two rather complex neuroelectric phenomena that subsequently were observed in neurons.[11],[15] It predicted the possibility of enhanced excitatory synaptic responses at one region of a neuron as a result of previous synaptic activity at a nearby region. This phenomenon was found by Kandel and Tauc.[17] The model also predicted the occurrence of periodic spikes with multimodal interval distributions, a phenomenon observed by Bishop, Levick, and Williams.[18] The quantitative as well as qualitative agreements between neuroelectric activities simulated in the model and those observed in neurons have given us sufficient confidence to extend the application of the model to systems more complex than a patch of neuronal membrane.

The main body of this paper describes the results of studies in which several of the electronic models were used to examine possible neuroelectric interactions among spatially distributed regions of a single neuron and neuroelectric activities in very small neural nets. Section II describes experiments in which six or more of the circuits were used as shunt elements in a lumped approximation to a finite length of axon. For the first time, the Hodgkin-Huxley model is extended to predict nonuniform conduction phenomena. Section III describes experiments in which two of the circuits are connected to form a two-patch model and used to examine the interactions in a single neuron

between a spike-generating region and a nonspiking region. Section IV describes studies in which a pair of two-patch models were used to examine signal-processing possibilities in four basic configurations of a pair of neurons.

The electronic models used in these studies were large and expensive to construct. Each model comprised 46 transistors and their associated circuits. Fifteen parameters of the Hodgkin-Huxley model and six synaptic parameters were controlled by variable resistors and capacitors. The complete circuit details of the model have been published elsewhere.[16],[19]

The size and complexity of the model have not proved disadvantageous for studies of very small neural networks; but model size, cost, and parameter management become limiting factors as larger nets are considered. For studies of slightly larger nets, a second model was designed with the same basic properties as the first but without the finer details and with much less elaborate provisions for parameter control. This model is described in Section V.

II. Modeling Neuroelectric Interactions Among Spatially Distributed Regions of an Axon

Most models dealing with its distributed properties treat the axon as a lossy cable, or core conductor, with active electrical properties. These active properties account for the attenuationless propagation of the spike. According to the Hodgkin-Huxley model, the active electrical properties, at least in the squid giant axon, are the result of the voltage-dependent potassium and sodium conductances. The distributed form of the Hodgkin-Huxley model has the same four shunt elements as the lumped form: membrane capacitance, leakage conductance, sodium conductance, and potassium conductance. In the lumped form, the element values were specified as magnitudes per unit area. In the distributed model they must be specified as magnitudes per unit length. This transformation is a simple one but requires knowledge of the ratio of axon-membrane area to axon length. In addition to the four shunt elements, the distributed Hodgkin-Huxley model includes a series resistive element, representing the resistance of the axoplasm to currents flowing from one region of axon membrane to another. Assuming a cylindrical axon, Hodgkin and Huxley described the distributed form of their model by means of a partial differential equation:

$$\frac{a}{2R}\frac{\partial^2 V_M}{\partial x^2} = C_M\frac{\partial V_M}{\partial t} + G_K(V_M - V_K) + G_{Na}(V_M - V_{Na}) + G_L(V_M - V_L)$$

where a is the axon radius, R is the axoplasm resistance per unit length, V_M is the membrane potential, and x is the distance along the axon; the other symbols are defined in conjunction with Fig. 1. Assuming that the propagated spike travels with a constant velocity θ, and without changing shape, Hodgkin and Huxley reduced this partial differential equation to the following ordinary differential equation:

$$\frac{a}{2R\theta^2}\frac{d^2 V_M}{dt^2} = C_M\frac{dV_M}{dt} + G_K(V_M - V_K) + G_{Na}(V_M - V_{Na}) + G_L(V_M - V_L).$$

This equation or its equivalents has been examined by several people.[5],[20],[21] Because it is based on the assumption of a uniform wave, however, its solutions do not include nonuniform phenomena such as the development of a spike as it is conducted from a point of barely threshold stimulation or the decremental conduction of a potential from a point of subthreshold stimulation. Cooley and Dodge[22] used a finite-difference approximation to solve the partial differential equation without the assumption of uniform wave; but their published solutions did not include nonuniform conduction. Lieberstein[23] modified the Hodgkin-Huxley partial differential equation by including the effects of a series inductance, and his solutions include spike development but not decremental conduction. These results have been extended by means of the electronic model. With the electronic models employed as shunt elements and resistors as series elements, a six-lump approximation of the distributed squid axon was constructed (see Fig. 2). Each of the shunt elements in the axon model represented 0.25 cm^2 of squid-axon membrane. These were separated by 4000-ohm resistors. Based on Hodgkin and Huxley's estimate of 35 $\Omega \cdot$ cm for axoplasm resistivity,[5] the lumped model represented a section of squid axon 4 cm long and 1 mm in diameter. This axon model was used to examine several aspects of conduction, and a number of nonuniform conduction phenomena were observed.[16] Some of the results are summarized in the following paragraphs.

A. Conduction of Single Waves

The six-lump axon model was driven by single, 4-ms current pulses applied across the first of the six shunt elements (Fig. 2). This configuration approximated an axon driven from a point adjacent to a long, insulated region (such as the regions adjacent to the patches of voltage-clamped membrane in the Hodgkin-Huxley experiments). Typical results are shown in Figs. 3(a) and 4. The oscilloscope traces in the photograph of Fig. 3(a) show the responses of the model axon to a subthreshold stimulus. The conduction in this case was decremental (i.e., the waveform was attenuated as it progressed along the model axon). The traces from top to bottom show the simulated intracellular potentials taken at nodes 1 through 6, respectively (see Fig. 2). The top trace thus shows the potential at the point of stimulus application, and the remaining traces going from top to bottom represent nodes progressively more remote from the point of stimulation. If the conduction time is taken to be the interval between the time of maximum depolarization at node 1 and the time of maximum depolarization at node 6, one can see that it is slightly more than 4 ms. The electrically excitable conductances (i.e., the potassium and sodium conductances) were removed from each of the six shunt elements, leaving a completely passive system.

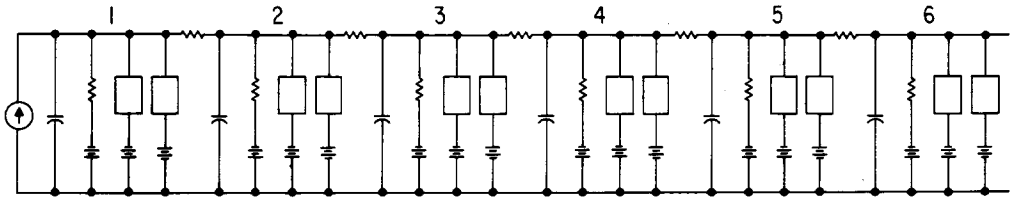

Fig. 2. A six-lump approximation to a section of axon. The four shunt elements in each lump represent the admittances of the Hodgkin-Huxley model. The series resistors represent the resistance of intracellular current paths. Electronic models simulated the shunt elements in this configuration, and the array was driven by a current source (shown at the extreme left).

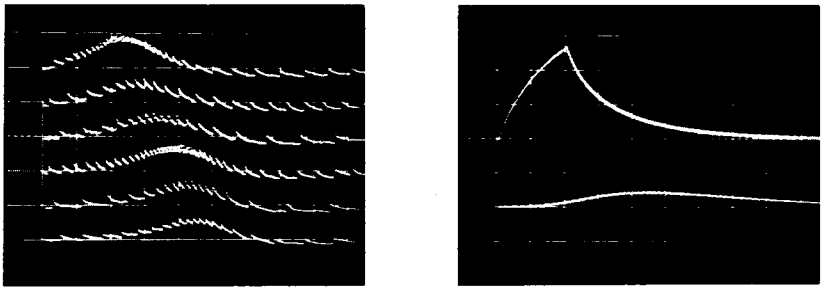

Fig. 3. (a) Response of the six-lump axon model to a subthreshold current pulse applied at node 1. From top to bottom the traces show the potentials at nodes 1 through 6, respectively. The serrations on the oscilloscope traces are superfluous but unavoidable results of the method of multiplication employed in the models. The time- and voltage-dependent conductances were simulated by frequency modulation of 1-μs pulses (see Lewis[19]). (b) Responses at nodes 1 and 6 to a current pulse applied at node 1 after the voltage-dependent conductances were removed from the model. Scales: major vertical divisions represent 20 mV; major horizontal divisions represent 2 ms.

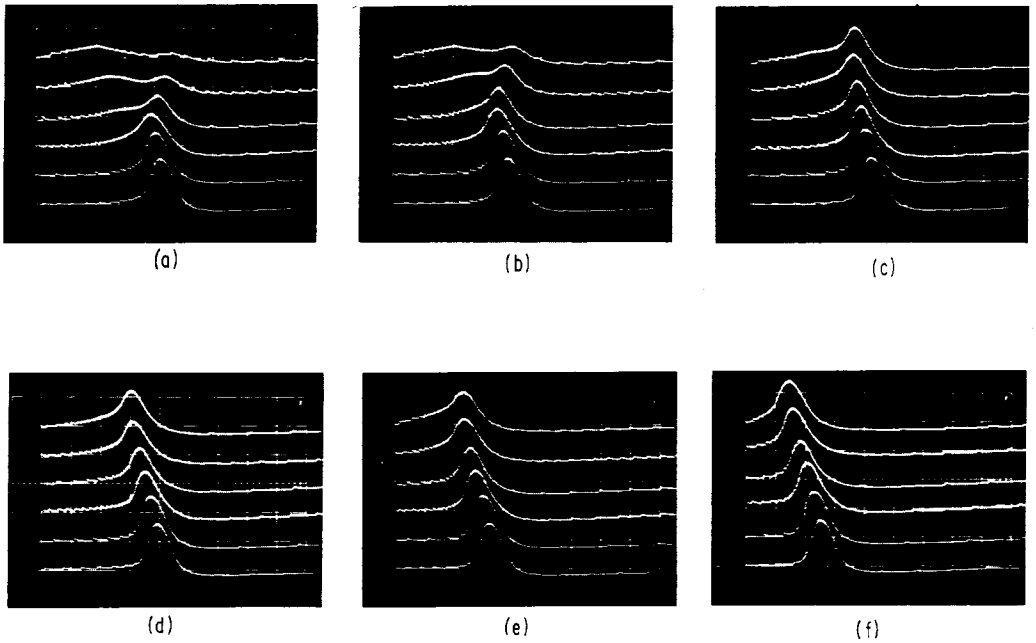

Fig. 4. A series of photographs showing the development of spikes in the six-lump axon model. The top trace in each photograph shows the potential at the point of stimulus application. The remaining traces, top to bottom, show potentials progressively more remote from the point of stimulation. From (a) through (f) the magnitude of the stimulus was progressively increased. Scales: major vertical divisions represent 50 mV; major horizontal divisions represent 2 ms.

Fig. 3(b) shows the responses at nodes 1 and 6 of this system to a 4-ms current pulse with five times the intensity of that applied in the case of Fig. 3(a). The axon model without electrically excitable conductances exhibited considerably more attenuation than its counterpart with excitable conductances, so the response in Fig. 3(a) was due largely to the regenerative action of the excitable conductances. The results illustrated in Fig. 3(a) are typical of those found throughout this study. Subthreshold potentials in the axon models, with their excitable conductances, exhibited nearly the same conduction times as potentials in their purely passive counterparts. The potentials in the excitable axon models, on the other hand, exhibited less attenuation and less tendency to prolongation or spreading as they were conducted. The reduced attenuation was almost certainly the result of the regenerative action of the simulated sodium conductance; the reduced spreading probably was the result of sharpening of the leading edge by the increasing sodium conductance and sharpening of the trailing edge by the increasing potassium conductance and decreasing sodium conductance.

Each of the photographs in Fig. 4 shows a potential developing into a spike as it was conducted along the axon model. Here again the top trace in each photograph shows the potential at the point of stimulus application; the remaining traces, top to bottom, represent nodes progressively more remote from the point of stimulation. Fig. 4(a) through (f), respectively, shows the effects of progressively increased stimuli at node 1. In Fig. 4(a) the stimulus initiated a slowly conducting potential that did not develop into a full spike until it reached node 4. The spike at node 4 was conducted in two directions: forward (orthodromically) with increased velocity and without attenuation, and backward (antidromically) without as much increase in velocity and with considerable attenuation (due to refractoriness at nodes 1 through 3). As the stimulus intensity was increased, the spike developed at nodes progressively less remote from the point of stimulation, and the antidromic spike reflections became larger and larger. Beginning with Fig. 4(d), the spikes at node 1 appear to have preceded those at node 2, so conduction probably was completely orthodromic. The conduction velocity is obscured, however, by the late occurrence of the spike at node 1. Conduction in the case of Fig. 4(f) appears to have reached steady state by node 3, and the conduction time from node 3 to node 6 was 1.4 ms. Since the model represented a 4-cm section of axon, the modeled conduction velocity was 17 m/s. This is comparable to the spike conduction velocities (14 to 23 m/s) measured in the squid giant axons.[5],[24]

B. Conduction of Repetitive Waves

When a sufficiently large, steady, depolarizing current was allowed to flow across any of the six shunt elements of the axon model, the potential across that element exhibited oscillations. When the depolarizing current was small, these oscillations were approximately sinusoidal; when the current was slightly larger, the oscillations were more nearly saw-toothed in appearance; when the current was even stronger, periodic spikes occurred. The mechanisms underlying the oscillations are described by Lewis.[11] Periodic waveforms of these types were induced by dc currents applied at node 1, and their conduction along the axon model was observed. Perhaps the most interesting result occurred in the case of conducted subthreshold oscillations. As in the case of single subthreshold waves, subthreshold oscillations were attenuated as they progressed from node 1 to node 6; but unlike the peaks of single waves, the peaks of the oscillations regularly occurred earlier in the nodes remote from their point of origin. In other words, they exhibited increasing phase lead as they were conducted along the axon model (see Lewis[16]). This phenomenon depended on amplitude; oscillations whose amplitude was less than approximately 10 mV exhibited progressive phase lag similar to that shown in Fig. 3, but larger oscillations exhibited phase lead. Occasionally oscillations would be attenuated past the critical voltage as they were conducted, gaining in phase up to one of the middle nodes and losing in phase beyond it. The mechanisms in the Hodgkin-Huxley model which underlie phase lead are discussed by Lewis.[16] Briefly stated, the frequency of oscillations induced in the shunt elements increased as the amplitude of oscillation decreased. Oscillations induced at node 1 elicited sympathetic oscillations at adjacent nodes, but these oscillations were reduced in amplitude and therefore tended to be of higher frequency. Thus, while the actual frequency of the sympathetic oscillations was forced to be identical to the frequency at node 1, the tendency toward higher frequencies resulted in phase lead. When the oscillations were attenuated sufficiently, they no longer elicited sympathetic oscillations. Conduction then became purely passive and decremental, and progressive phase lead gave way to progressive phase lag. The photograph in Fig. 5 shows the oscillatory potentials in the axon model immediately after the onset of the depolarizing current at node 1. The first wave is conducted from node to node in the normal decremental manner, with progressive delay. The second wave appears to be conducted without any delay at all. At nodes 3 through 6, the amplitude of the second wave is conspicuously larger than that of the first, exhibiting the effects of the sympathetic oscillation. Conducted periodic spikes were never seen to exhibit phase lead, and when periodic subthreshold oscillations occasionally evolved into full spikes, phase lead was replaced by progressive phase lag (see Fig. 6).

C. Spike Collisions and Circus Conduction

An eight-lump axon model was constructed with 10-kΩ internodal resistors. The shunt elements were identical to those in the experiments described in Section II-A and B. Fig. 7 shows the potentials at all eight nodes when spikes were initiated by simultaneous stimuli at nodes 1 and 8. The spikes collided at node 5 and were annihilated. Spike collision and annihilation have been discussed by Crane[25] in regard to his neuristor studies, and by Lillie[26] and

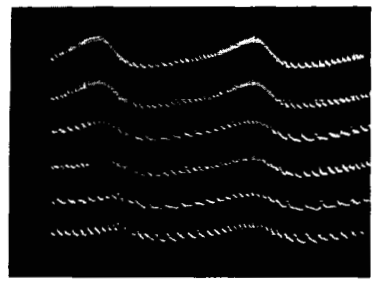

Fig. 5. Transient onset of conducted subthreshold oscillations in the axon model. Oscillations were induced at node 1 (top trace) and conducted to node 6 (bottom trace). Scales: major vertical divisions represent 20 mV; major horizontal divisions represent 5 ms.

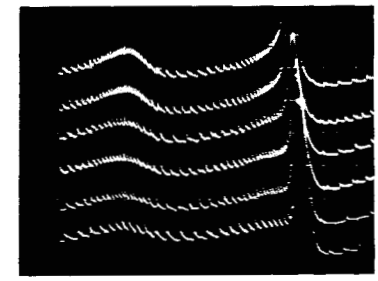

Fig. 6. Conducted subthreshold oscillations interrupted by a spike. The oscillations were induced at node 1 (top trace) and conducted to node 6 (bottom trace) with no visible delay. When the oscillation at node 1 developed into a spike, the latter was conducted to node 6 with noticeable delay. Scales: major vertical divisions repesent 20 mV; major horizontal divisions represent 5 ms.

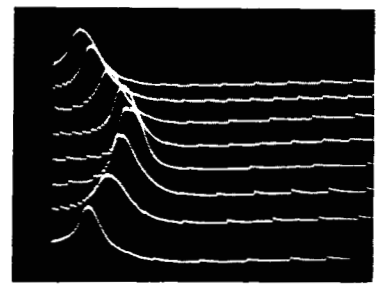

Fig. 7. Spikes colliding in an eight-lump axon model.

Fig. 8. Spikes conducted around a continuous ten-lump axon model. From top to bottom, traces show potentials at nodes 1, 3, 5, 7, and 9, respectively. Node 10 was connected back to node 1.

others in regard to iron wire models of axons. Kennedy and Mellon[27] have discussed the possibility of collision and annihilation being a useful phenomenon in the crayfish nervous system.

Fig. 8 shows the potentials at five alternate nodes of a ten-lump axon model. In this case node 10 was connected back to node 1 through a resistor in series with a diode. The diode ensured that a spike originating at node 1 would propagate in only one direction (i.e., to nodes 2, 3, 4, etc., not to nodes 9, 8, 7, etc.). In Fig. 8(a) a spike initiated at node 1 propagated once around the loop but failed to conduct past node 9 on the second time around. In Fig. 8(b) the spike continued around the loop, periodically passing each of the ten nodes. Circus conduction of this type has been observed in living preparation by Wilson,[28] Furshpan and Potter,[29] and others, but it has involved two fibers with either electrical connections or synapses. Lillie[26] produced circus conduction in a ring of iron wire immersed in nitric acid, and Crane[30] has based some of the operation of neuristor circuits on circus conduction.

III. Modeling Neuroelectric Interactions Between Integrative and Trigger Regions

The dendrites and somata of many neurons are capable of completely graded electrical activity, exhibiting no threshold and no spikes (see Bullock and Horridge,[31] pp. 186, 189, 234). These are the regions that usually receive synaptic inputs from other neurons, and their ability to respond in a graded manner allows them to sum the inputs smoothly. Occasionally the membrane potentials in these regions exhibit pacemaker potentials that produce periodic spikes or periodic changes in excitability along the axon.[10] The parts of a neuron capable of graded response often are called integrative regions; the parts nearest them (usually along the axon) capable of generating spikes often are called trigger regions. The summed electrical events in the integra-

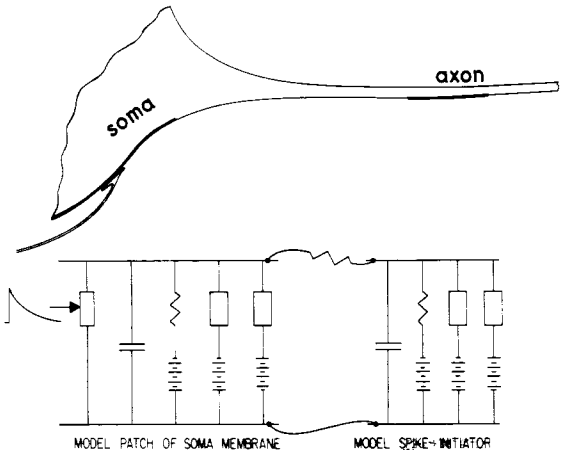

Fig. 9. A two-patch representation of a neuron. The model on the left represents an integrative region of a nerve cell; the model on the right represents a trigger region. The resistor between them represents the resistance of intracellular current paths from one region to the other. The shunt element on the extreme left represents an excitatory synaptic conductance, which is modulated by decaying exponential waveforms. The remaining shunt elements represent the admittances specified by Hodgkin and Huxley.

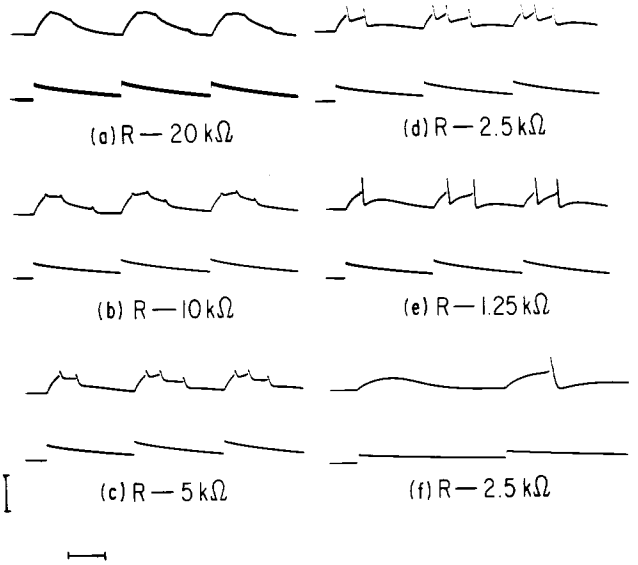

Fig. 10. Invasion of the integrative region by spikes generated at the trigger region. The upper trace in each pair shows the simulated internal soma potential of a two-patch model receiving simulated excitatory synaptic inputs. The time course of the simulated synaptic conductance is shown in the lower trace. The initial conductance increments were 0.1 millimho. Scales: vertical line represents 20 mV; horizontal line represents 50 ms.

tive region long have been presumed to initiate spikes in the trigger region and thus to a great extent to determine the neuron's output. Many modeling studies have taken this effect into account. Spikes in the trigger region, on the other hand, will not be unfelt at the integrative regions. Pacemaker potentials, for example, may be reset by the effects of spikes at remote trigger regions.[32],[33] As far as I know, the two-way interactions of an integrative region and a trigger region have not been modeled previously. A two-lump approximation to a spatially distributed neuron is the simplest configuration that will provide such interactions. The following paragraphs describe some experiments in which the electronic models were used as the shunt elements in the two-patch representation of a neuron illustrated in Fig. 9.

Throughout these studies, the integrative patch was taken to be capable only of graded response and incapable of producing a spike. In the simulation of this patch, all but one of the parameters of the electronic model were set to the values specified by Hodgkin and Huxley. The single difference was the simulated transmembrane capacitance, which was set at magnitudes eight to twenty times the specified value. With the larger values of membrane capacitance, the electronic model was capable only of completely graded response. Membrane capacitances of these magnitudes have been measured in several integrative neural somata[12]–[14] so this seems to be a reasonable parameter adjustment. All of the parameters of the electronic model representing the trigger region were set to the values specified by Hodgkin and Huxley.

In the system of Fig. 9, a slow positive-going potential, such as a prolonged excitatory postsynaptic potential (EPSP) at the soma, presumably can elicit spikes along the axon, and the occurrence of an axonal spike should have some effects at the soma. A typical experiment to determine these effects is shown in Fig. 10. The nonspecific shunt conductance of the soma model was modulated by a series of three decaying exponentials (lower trace of each pair). The transient conductance changes induced simulated EPSP's in the soma model (upper trace in each pair), and these in turn elicited spikes at the model trigger region. The reflections of the spikes can be seen superimposed on the EPSP's. From Fig. 10(a), the resistance between the soma model and the model trigger region was progressively reduced from 20 kΩ to 1.25 kΩ. In Fig. 10(a), two spikes were elicited by the first EPSP and three spikes each by the second and third EPSP's. The miniature, reflected spikes are barely visible on the EPSP's and apparently did not alter their form. In Fig. 10(b) the spike reflections were larger, but do not appear to have altered significantly the EPSP's. Three spikes occurred on the first EPSP, and the spikes on the second and third EPSP's occurred earlier than in the case of Fig. 10(a); the EPSP's in Fig. 10(b) thus seem to have been more effective in eliciting spikes. In Fig. 10(c) the invading spikes tended to polarize, or reset, the soma potential; so in spite of the fact that the coupling resistance was less than in the case of Fig. 10(b), the EPSP's were less effective in eliciting spikes. This is evident from the fact that only two spikes occurred on the first EPSP, and the spikes on the second and third EPSP's occurred later than they did in Fig. 10(b). In Fig. 10(d) and (e) the resetting of the soma potential was even more pronounced. Fig. 10(e), in fact, shows only one spike on the first EPSP and two each on the second and third EPSP's. Fig. 10(f) shows the resetting of the soma potential by a single spike on the second EPSP. The effects of the two EPSP's probably were summed at the trigger region, so the second potential was able to elicit a spike. The time

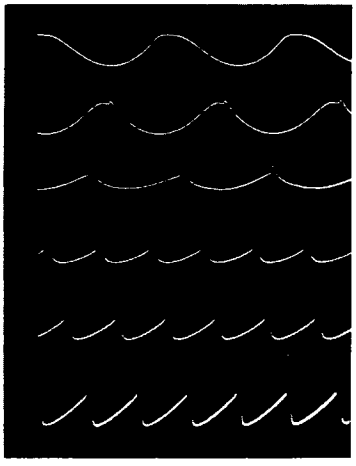

Fig. 11. Reflected spikes resetting pacemaker potentials in an integrative region. From top to bottom, the traces show the effects of progressively stronger coupling between the integrative region, where the oscillations originate, and the trigger region, where they elicit spikes.

scale was expanded in this photograph to show the resetting in more detail.

In a second type of experiment positive dc currents were applied to the soma model. These produced oscillations such as those shown in the top trace of Fig. 11. In this case the coupling (20 kΩ) between soma and trigger region was too weak to allow the oscillations to elicit spikes. In the case of the second trace, the coupling resistance was halved, allowing spikes to occur on the positive phases of the oscillations. Miniature reflections of these spikes can be seen on the oscillations at the soma. The occurrence of these spikes appears to have altered slightly the shape of the oscillations without much affecting their frequency. In the case of the third trace, the coupling resistance was halved again. The amplitude of the oscillations and their frequency were both altered noticeably by the spikes. The fourth, fifth, and sixth traces show the effects of further halving of the coupling resistor. In the bottom trace, the resistance was 612 Ω. The oscillations that were nearly sinusoidal in the top trace are nearly saw-toothed in the bottom trace. Resetting of the soma potential by the reflected spike has increased the frequency of oscillation from 15 Hz in the top trace to 44 Hz in the bottom trace.

The results of this study indicate that in cases of moderate to strong coupling between an integrative region and a trigger region, each having voltage- and time-dependent conductances conforming to the Hodgkin-Huxley model, the effects of spikes reflected to the integrative region will be significant. Because they depend entirely on the voltage-dependent conductances of the integrative region, pacemaker potentials are very susceptible to invading spike reflections. Synaptic conductances, on the other hand, are independent of membrane potential; so synaptic potentials are not as susceptible to spike reflections. This difference has been observed in the lobster cardiac ganglion, where as many as four spike reflections may occur on a single EPSP,[7] but a maximum of one reflected spike occurs on a single pacemaker oscillation.[32] The extent of the neuroelectric interactions between integrative and trigger regions of course will depend on their relative sizes. A larger integrative region will be considerably less affected by spikes than a small region will be. Two-patch models with larger simulated soma areas than that in the case of Fig. 11 were able to develop several spikes on each pacemaker cycle.[16] In addition, a region with larger membrane capacitance will be more immune to spike reflections. The electronic model would not produce pacemaker oscillations, however, when its capacitance was equal to or greater than twenty times that specified by Hodgkin and Huxley.

IV. Modeling Neuroelectric Interactions Between a Pair of Neurons

A neuron may be connected to another neuron in one or more of three basic ways—with an excitatory chemical synapse, with an inhibitory chemical synapse, or with an electrical connection. The chemical synapses are unidirectional, but the electrical connection presumably is necessarily bidirectional. Parts A, B, and C of this section describe experiments in which a pair of two-patch models were interconnected with three combinations of simulated synaptic coupling. The two-patch models themselves were slightly different from those described in Section III. The electronic model was used for the integrative patch, but the trigger region was represented by the simplified circuit described in Section V. In Part D of this section, some of the effects of purely electrical connections are described. Most of the experiments in these cases were performed with one-patch models representing only the trigger regions of the simulated neurons.

A. Mutual Inhibition

The effects of mutual inhibition have been examined by several modelers; in fact, the most thoroughly studied small nerve net probably is the reciprocally inhibiting pair.[15] The recent resurgence of these studies began with Reiss,[34] who found that a pair of mutually inhibiting point models could respond to a common, pulsed driving source by producing periodic bursts of spikes. The models alternated, so that while one was generating spikes, the other was quiescent. Reiss included simulated fatigue in his models, and this limited the duration of each single burst, making alternation possible. The simulated synaptic time constants in Reiss's models were quite long, usually 100 ms or more. Harmon[35] studied mutual inhibition in nearly identical models, but without simulated fatigue and with shorter synaptic time constants. He found stable spike patterns that depended on the intensity of the common, pulsed driving source, but most of these patterns comprised alternate spikes or small groups of spikes rather than long bursts. Harmon also noted hysteresis in the transitions between these patterns. In a similar study, Wilson[36] found stable alternate production of single spikes by mutually inhibiting models. This alternation of single spikes occurred over a wide range of input intensity, and the principal effect of increased intensity was increased frequency of the

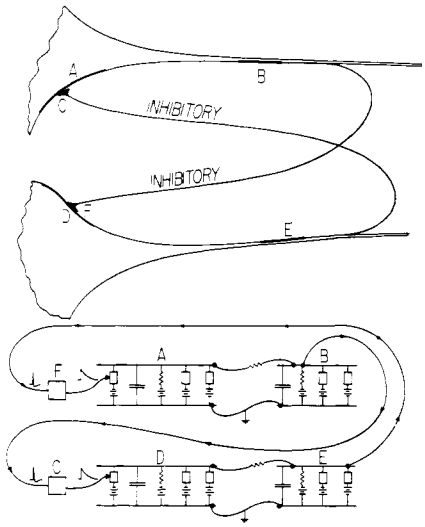

Fig. 12. A model of a mutually inhibiting pair of neurons. Corresponding points in the upper and lower figures are designated by the same letter. The two-patch models are similar to that shown in Fig. 9, but the element on the extreme left in each model represents the synaptic component of potassium conductance rather than the nonspecific shunt conductance.

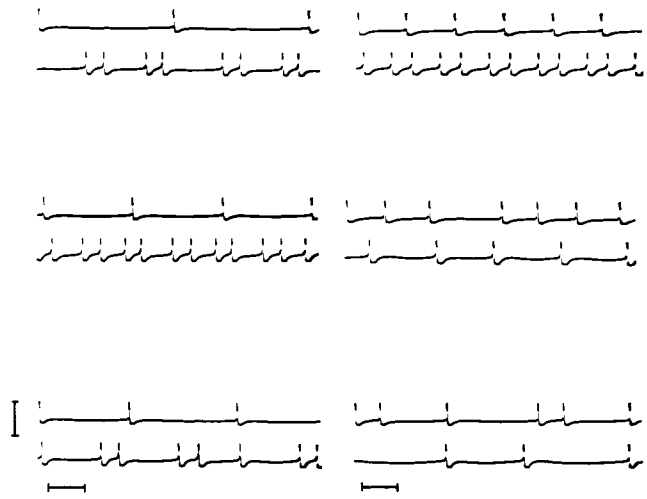

Fig. 13. Spike patterns at the trigger regions of a pair of mutually inhibiting two-patch models. Scales: vertical line represents 100 mV; horizontal lines each represent 200 ms.

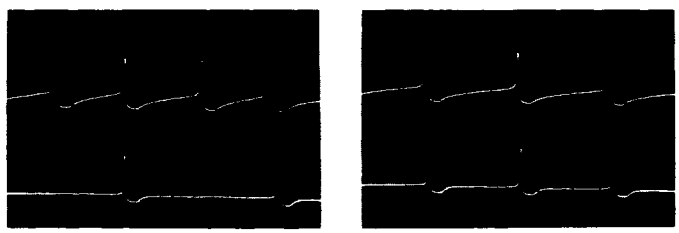

Fig. 14. Synchronous spikes from a pair of mutually inhibiting two-patch models.

same pattern. In each of these three studies, both members of the reciprocally inhibiting pair were driven by a single, periodic pulse source. In spite of the fact that the input pulses applied to one member thus were synchronous with those applied to the other member, most of the output spike patterns observed in reciprocal-inhibition studies have been patterns of alternation and exclusion, not patterns of synchrony or near synchrony. When synchrony did occur among output spikes, it depended completely on the presence of a common, pulsatile input source. In our studies with the two-patch models, on the other hand, stable patterns with spike synchrony were quite common in mutually inhibiting pairs that were driven with independent, nonpulsatile sources. The following paragraph describes one such study.

A pair of two-patch models were connected as shown in the configuration of Fig. 12; the soma capacitances both were eight times the Hodgkin-Huxley value. The spikes from each trigger model were converted to decaying exponentials that modulated the synaptic component of potassium conductance at the soma of the other two-patch model. By means of the modulated potassium conductance, each spike produced a simulated inhibitory postsynaptic potential (IPSP) at the soma of the receiving model. Propagation delay was not simulated in these experiments, so the effect of the spike on the conductance was almost immediate. Before the inhibitory connections were made, a steady depolarizing current was applied to the simulated soma of each two-patch model, producing subthreshold oscillations at the somata and periodic spikes at the trigger regions. When the connections were made, the patterns changed from periodic spikes to periodic groups of spikes, such as pairs or unevenly spaced triplets. Typical patterns are shown in Fig. 13. The asymmetries between the top and bottom traces were due partly to differences in synaptic time constants; the IPSP's were longer and thus more effective in the model represented by the top trace. In addition, the depolarizing currents were varied at the somata of the two-patch models, accounting for the pattern variation. The patterns shown in Fig. 13 were extremely stable, and at least one period of each pattern is shown. The longest pattern shown is in the lower left-hand pair of traces. One unit produced three nonuniformly spaced spikes, while the other unit produced two single spikes and two pairs of spikes. Most of the patterns in Fig. 13 exhibit nonsynchronous generation of spikes by the two models, but the pattern on the lower left and that on the lower right both exhibit spike synchrony. Synchrony actually was very common with the mutually inhibiting two-patch models. Fig. 14 shows two more examples from the same test configuration.

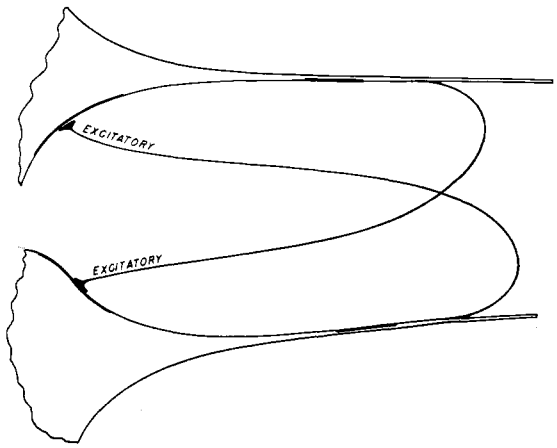

Fig. 15. Diagram of a pair of mutually exciting nerve cells.

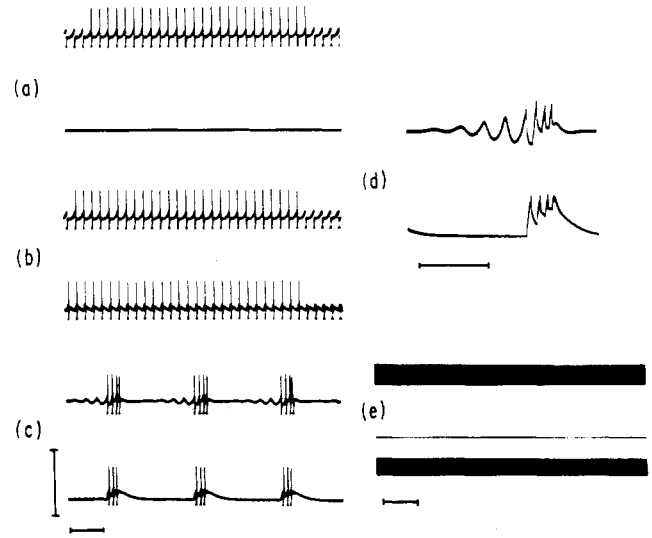

Fig. 16. Potentials from a pair of mutually exciting two-patch models. (a) Spontaneous unit firing alone (upper trace). (b) Spontaneous unit (upper trace) driving second unit (lower trace). (c) Mutually exciting pair. (d) Potentials at integrative regions of mutually exciting pair. (e) Runaway due to increased synaptic efficiency. Scales for (a), (b), (c), and (e): vertical line repesents 100 mV; horizontal lines each represent 200 ms.

Synchrony in these cases was essentially complete; when spikes occurred in both two-patch models, they occurred in synchrony.

Perkel *et al.*[37] considered a nondistributed neuron model producing spontaneous, periodic spikes and receiving periodic inhibitory synaptic inputs from another neuron. They showed that stable phase-locking could occur between the inhibitory inputs and the spikes of the spontaneous cell. It can be shown by similar considerations that if the effect of each inhibitory input is delayed sufficiently, stable spike synchrony can occur between mutually inhibiting, spontaneous neurons.[38] In the models employed by Reiss, Harmon, and Wilson, the occurrence of a spike in one member of the mutually inhibiting pair excluded almost immediately the possibility of a spike in the other member. In the two-patch model, both the integrative nature of the soma model and the fact that simulated synaptic coupling was mediated by a conductance change rather than an abrupt change of membrane potential tended to delay the effect of an inhibitory input. This delay was sufficient to allow spike synchrony.

B. Mutual Excitation

The soma capacitance of each member of a pair of two-patch models was adjusted to eight times the Hodgkin-Huxley value. The models were connected in a configuration identical to that of Fig. 12 in every respect but one: the modulated conductance was the nonspecific shunt rather than the potassium conductance. The simulated synaptic potentials therefore were excitatory rather than inhibitory. When the models were connected in this manner, they represented the configuration of Fig. 15. The oscilloscope traces in Fig. 16 show the simulated intracellular potential of the trigger regions of both models. The pair of traces in Fig. 16(a) were photographed before the synaptic connections were made. A steady depolarizing current had been applied to the soma of one model, causing its trigger region to produce periodic spikes at a frequency of approximately 18 Hz (top trace). The model producing the periodic spikes was coupled to the quiescent unit by means of the simulated excitatory synaptic connection. The amplitude of the synaptic conductance increment at the driven model (represented by the lower trace) was adjusted to a magnitude that was barely sufficient to allow the driven model to produce one spike for each spike from the driving unit (upper trace), as shown in Fig. 16(b). The synaptic conductance increment of the driving model was adjusted to approximately the same magnitude as that in the driven model, and the driven model was coupled back to the driving model through a simulated excitatory synapse. The loop with mutual excitation was now complete.

The spike outputs of the two mutually exciting models are shown in Fig. 16(c). The models produced the spikes in periodic bursts. The maximum spike frequency during a burst was approximately 50 Hz, representing a considerable acceleration of the frequency of 18 Hz which existed before the excitation loop was closed. The frequency of bursts was about 2 Hz, and the interburst interval (i.e., the period of quiescence between bursts) was approximately 400 ms, considerably longer than the interspike interval before the excitation loop was closed. The simulated intracellular potentials at the two soma models during a burst are shown in Fig. 16(d). The growth of subthreshold oscillations during the interburst interval in the driving unit can be seen in the top trace. The first spike at the trigger region of the driving unit reset its soma potential, originating a burst and terminating the oscillation. The soma potentials in both models during the burst were combined EPSP's and reflected spikes. The effect of increased synaptic efficiency in this system can be seen in Fig. 16(e). The synaptic conductance increment per presynaptic spike was increased in each model. Rather than burst production, the mutually exciting pair now exhibited complete runaway, both models producing spikes at frequencies of approximately 100 Hz. With the mutually exciting pair of models adjusted to produce

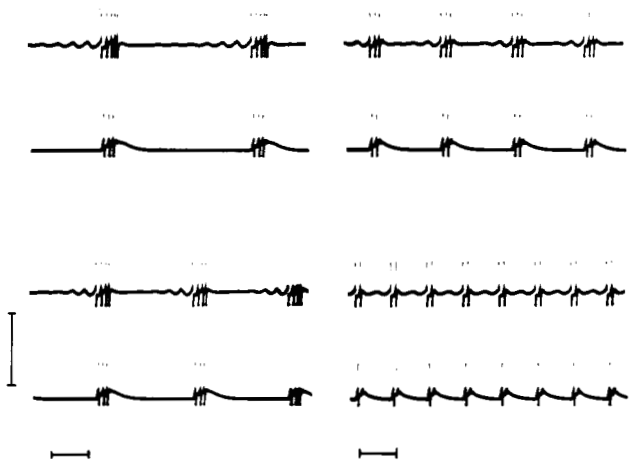

Fig. 17. Bursts of spikes from a mutually exciting pair of two-patch models. Scales: vertical line represents 100 mV; horizontal lines each represent 200 ms.

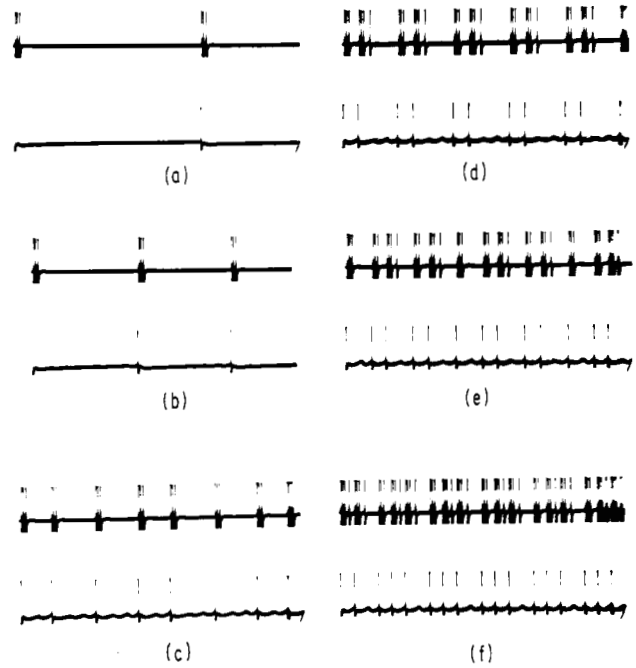

Fig. 18. Spike patterns from a pair of two-patch models. The spontaneous unit (lower trace of each pair) excited the second unit (upper trace), which in turn inhibited the spontaneous unit.

bursts of spikes, the dc current at the soma of the driving model was varied. The results are shown in Fig. 17. As the current was increased, the frequency of bursts increased and the number of spikes per burst decreased.

Two types of process were required to convert the periodic spike trains of Fig. 16(a) and (b) to the periodic bursts of Figs. 16(c) and 17: an accelerating process and a quenching process. During the bursts, spike production was accelerated from 18 Hz to nearly 50 Hz. These bursts were terminated or quenched, however, and the trigger regions were quiescent for an interval during which several spikes would have occurred under normal conditions (i.e., if the models were producing periodic spike trains rather than bursts). The accelerating process in the mutually excitatory configuration is obvious. The mutually excitatory synaptic coupling provides positive feedback in the system. If the acceleration due to mutual excitation were not arrested, however, complete runaway such as that shown in Fig. 16(e) would occur. Complete runaway is prevented by the quenching process. It is obvious from the upper trace of Fig. 16(d) that the first spike in the driving model invaded its soma and reset the oscillatory potential there. While this resetting of the soma potential may have been part of the quenching process, it cannot have been all of it, since the spike generation continued to accelerate after the soma potential had been reset. As a test of the necessity of invasion of the soma by reflected spikes for quenching, the soma potential was applied through an isolation amplifier to the trigger region. Thus, while the soma potential was conducted to the trigger just as before, the trigger and its spikes had absolutely no effect on the soma potential. The models continued to produce bursts with very little difference from those produced in the original configuration. Invasion of the soma by spikes was therefore not an essential part of the quenching process. Although antidromic spikes were blocked, the soma potential was nonetheless reset, but by EPSP's rather than spikes. Resetting of the soma potential by one means or another probably was an essential part of quenching. Another essential part of quenching apparently was refractoriness in the trigger models. Because of the rapid succession of spikes, the variables that produce refractoriness had accumulated sufficiently to prevent the last EPSP from eliciting a spike. In Fig. 16(d) the spike failed on the fourth EPSP of the lower trace.

C. *Excitation and Inhibition*

Another set of simple connections between two neurons is the combination of excitation and inhibition. In the configuration discussed in this paragraph, spikes from the driving model excited the driven model, while spikes from the driven model inhibited the driving model. As in the previously discussed configurations, a steady dc current was applied to the soma of the driving model, inducing oscillations of the soma potential and periodic spikes at the trigger region (lower trace of each pair in Fig. 18). The spike from the driving unit elicited a short burst of spikes from the driven unit (upper trace in each pair). This burst in turn inhibited the driving unit. The dc current at the soma of the driving model was gradually increased, and the results of this increased current are shown in Fig. 18(a) through (f), respectively. If one were to look only at the driving model, he would see an interesting sequence of patterns as the dc current was increased. At low current levels he would see single, periodic spikes whose frequency increased with increasing current. As the current was increased further, he would see alternating spikes and spike pairs, then periodic spike pairs, then alternating spikes and spike pairs again and, finally, periodic spike triplets. The same patterns are reflected in the upper traces, but with short bursts replacing single spikes.

The spike patterns described in Section IV-A, B, and C are rather complex and diverse, yet they are the results of very simple connections between two very simple neural models. Each of the experiments described in these sections

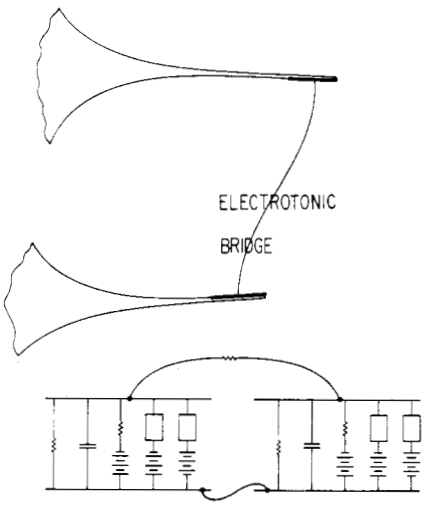

Fig. 19. Diagram of a pair of electrotonically coupled trigger regions.

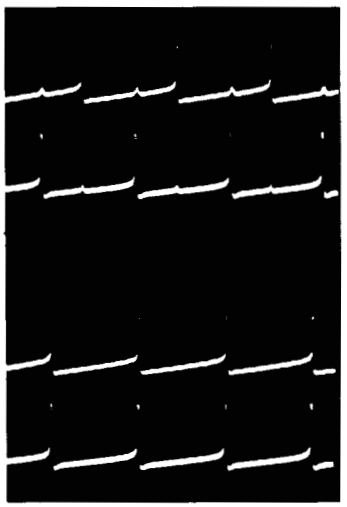

Fig. 20. Two modes of stable phase relationships between the same pair of electrotonically coupled trigger regions.

included systematic variation of only one parameter; but the two-patch model has many parameters, so one should expect much greater diversity and perhaps much greater complexity in the patterns actually available from these configurations.

D. Electrotonic Connections

Although communication from one nerve cell to another in most cases is thought to be mediated by a chemical transmitter, communication in a few cases is thought to be electrical, mediated by resistive coupling between the internal fluids of the two cells.[28],[33],[39] Evidence for electrical communication comes from electron micrographs and from physiological data. In the case of the former, the connections often are called tight junctions; in the case of the latter, they often are called *electrotonic* connections. In some cases, electrotonic connections are thought to be purely resistive; in others, they may exhibit distributed resistance and capacitance.[40] Functionally, there probably is very little difference between connections inherent among regions of a single cell and electrotonic connections among regions of different cells. The configuration in Fig. 2, for example, can represent electrotonically connected trigger regions from six different cells as well as it can represent an axon of one cell. Fig. 19, on the other hand, shows a configuration representing just two electrotonically connected trigger regions. The fifth element, a shunt resistor, in each model passes current sufficient to elicit periodic spikes. When the resistance connecting them is very small, the two models act as one, producing spikes in synchrony. As the connecting resistance is increased, the models become progressively more independent. The electronic models have been used to examine several configurations with electrotonic connections[16]; however, of all these configurations that of Fig. 19 has been studied most thoroughly.

The photographs in Fig. 20 show one of the results of weak electrotonic coupling between the two models in this configuration. Before the models were coupled, the magnitudes of their shunt resistors were adjusted until the spike frequencies were nearly equal. After connection of the coupling resistor, the spike trains held one of two stable phase relationships: stable synchrony or stable alternation. The upper two traces of Fig. 20 show the spike trains in stable alternation; the lower two traces show stable synchrony. A quantitative discussion of these models recently has been published.[41] The main point, however, is that in the case of spikes (such as those in the squid axon) that have both a positive and a negative phase, electrotonic coupling between trigger regions may be either excitatory or inhibitory. In the case of Fig. 20, when a spike in one unit occurred while the potential of the other unit was close to threshold, the two units fired in synchrony. When, on the other hand, the spike in one unit occurred too early to elicit a spike in the second unit, the negative phase in the first unit retarded the ascending potential of the second and prolonged the interspike interval. The electrotonically conducted spike thus is excitatory or inhibitory, depending on the state of the region to which it is conducted.

Borrowing from Section III, from my other modeling studies, and from modeling studies performed by Wilson,[36] I can propose several other general properties of electrotonic connections. 1) Electrotonic conduction of dc or low-frequency potentials is degenerative, always imposing attenuation and usually imposing phase lag. 2) Attenuation may be reduced, but not eliminated, when sympathetic oscillations are induced at the receiving end of the conducting path. 3) Phase lag may give way to phase lead in cases of sympathetic oscillation. 4) Electrotonic conduction between a pair of spontaneously firing (pacemaker) neurons can produce a tendency toward spike synchrony but cannot effect mutual acceleration of spike production. 5) Electrotonic conduction between pacemaker neurons can result in tendencies toward stable phase relations other than spike synchrony; but in most cases these tendencies are ephemeral, being strongly frequency-dependent and highly susceptible to parameter changes.[36],[41] 6) Electrotonic conduction between several trigger regions can produce, under very special conditions, acceleration of spike production by means of circus conduction, such as that illustrated in Fig. 8.

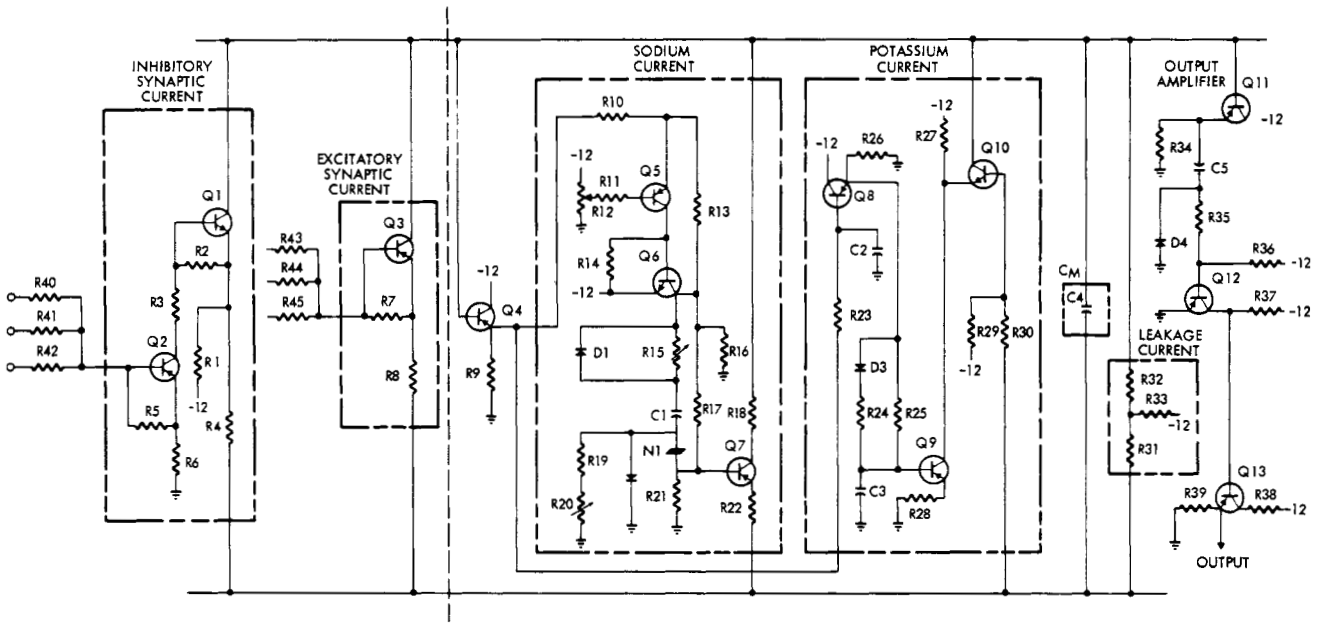

Fig. 21. A circuit designed to simulate a single patch of electrically excitable membrane (on the right of the vertical dashed line) with a contiguous patch of subsynaptic membrane (on the left of the vertical dashed line). Each subcircuit enclosed in a dashed box represents a shunt element across the neural membrane. The top of the circuit represents the inside of the membrane; the bottom represents the outside. Component values are given in Tables I and II.

V. Simplified Circuits for Studies of Larger Nerve Networks

Most of the experiments described in Sections II, III, and IV were performed with rather elaborate electronic circuits whose limitations are enumerated in Section VI. These models were very large and expensive to construct, and each included twenty-one parameter controls. As one considers larger neural nets, model size, cost, and parameter management become limiting factors. The model described in this section is proposed as a compromise between detailed realism on the one hand and reasonable cost and tractability on the other. These simpler models have been used successfully by themselves in several studies of neural networks (e.g., see Wilson[36] and Wilson and Waldron[44]). In addition, they have been employed as trigger regions in many of our studies with two-patch models (e.g., those of Section IV-A, B, and C of this paper).

The compromise between detailed realism and tractability led to two versions of the final design. One includes an approximate realization of the Hodgkin-Huxley model for relatively small excursions of membrane potential and is intended to simulate regions of a nerve cell where subthreshold activity is important. The other version, intended to simulate trigger regions, includes an approximate realization of the Hodgkin-Huxley model for large excursions of the membrane potential.

A. A Model for Trigger Regions

Fig. 21 is a schematic diagram of the basic electronic circuit. Dashed boxes in the figure surround each of six subcircuits, and a dashed line separates the synaptic portion of the circuit from the Hodgkin-Huxley portion. The six subcircuits in the figure are shown connected in parallel between two wires, one wire representing the inside of the membrane and the other representing the outside. Each of these subcircuits represents a shunt admittance across the nerve cell membrane. The four circuits to the right of the dashed line are approximations of the four elements of the Hodgkin-Huxley model. The two circuits to the left of the line are approximations of excitatory and inhibitory synaptic conductances. The seventh circuit, shown on the extreme right in Fig. 21, is a pulse-shaping amplifier that has no effect on the electrical properties of the simulated membrane patch. When a spike occurs across the membrane, this amplifier provides a square, negative-voltage pulse at its output terminal.

Although the circuit on the right of the dashed line is not intended to be a faithfully detailed analog of the Hodgkin-Huxley model, some quantitative comparisons can be made. First, in order to make the voltages compatible with the electronic elements in the circuit, the simulated membrane potential has been increased by a factor of 100. One volt in the circuit represents 10 mV in the Hodgkin-Huxley model. In addition, no provision has been made in the circuit for positive internal membrane potentials; so spikes are truncated at $V_m = 0$, and the normal spike amplitude in the circuit is 7 volts (equivalent to 70 mV in the neuron). Two of the four Hodgkin-Huxley elements can be simulated quite simply and accurately. The transmembrane capacitance is represented by the fixed capacitor $C4$; the membrane leakage conductance is represented by a fixed resistor $R32$. A voltage divider, $R31$–$R33$, provides the equilibrium potential for the leakage current. Being dependent on both the transmembrane potential and time, the remaining two elements of the Hodgkin-Huxley model are more difficult to simulate. In this circuit we have attempted to approximate

the potassium and sodium ion currents with subcircuits which are inexpensive and compact but which, nonetheless, provide currents resembling those of the Hodgkin-Huxley model. By means of Fig. 22, we can compare the currents in response to positive voltage steps in the circuit to those in the squid giant axon according to Hodgkin and Huxley.

First, consider the sodium current I_{Na}. The sum of the delay and rise times of the sodium current is much less than the time constant of the resting membrane, so they have been neglected in the circuit, where they are essentially zero. The peak magnitude of the sodium current in the Hodgkin-Huxley model is a very nonlinear function of ΔV_m. The simulated dependence in the circuit is compared to it in Fig. 23. The decline or inactivation of the sodium current in the squid axon is nearly exponential. The time constant decreases monotonically with increasing values of ΔV_m, varying from more than 6 ms to approximately 0.6 ms. In the circuit, the time constant of inactivation is nearly constant at 0.6 ms. Following repolarization of the squid-axon membrane to the equilibrium potential, the sodium current declines very rapidly toward its equilibrium value. In the circuit, the time constant of this decline is neglected and is essentially zero. When a second step voltage is applied to the squid axon soon after repolarization from the first step, the peak magnitude of the sodium current increases approximately exponentially with the interval between the repolarization and the subsequent step. Hodgkin and Huxley determined the time constant for one case: it was approximately 12 ms for $\Delta V_m = 44$ mV. The corresponding time constant in the circuit is variable, being determined by resistor $R15$.

The rise of the squid-axon potassium current is sigmoid and considerably slower than that of the sodium current. The delay and rise times generally decrease with increasing ΔV_m, the delay time varying from more than 2 ms for small ΔV_m to less than 1 ms for large ΔV_m and the rise time varying from more than 10 ms to approximately 2 ms. In the circuit, the rise of current is sigmoid, but the delay and rise times are constant at approximately 1 ms and 2 ms, respectively. In the squid axon, the final value of potassium current increases monotonically with increasing ΔV_m; the corresponding current in the circuit is directly proportional to ΔV_m. The squid-axon and the potassium circuit currents are compared in Fig. 24. On repolarization of the squid axon to the resting potential, the potassium current falls approximately exponentially with a time constant of 5 to 10 ms. The decline of simulated potassium current in the circuit is exponential, and the time constant is fixed at 10 ms.

The two subcircuits on the left side of the dashed line complete the model. They provide currents similar to the synaptic currents in nerve cells. The inhibitory synaptic circuit produces a negative current proportional to the sum of the voltages applied to the input resistors. This current approaches zero as the simulated membrane potential approaches -8 volts (corresponding to -80 mV in a neuron). The excitatory synaptic circuit produces a positive current proportional to the sum of the voltages applied to the input resistors. The excitatory synaptic current approaches zero as the simulated membrane potential approaches zero.

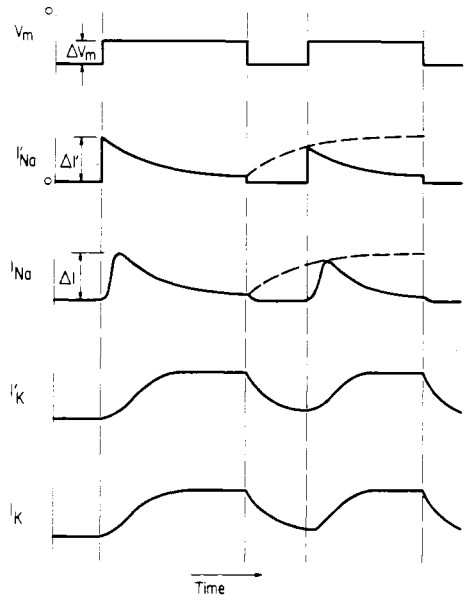

Fig. 22. Simulated ionic currents in the circuit of Fig. 21 and their prototypes in the squid giant axon.[5] The currents are in response to the stepwise change in membrane potential shown on the top line. The simulated sodium current (I'_{Na}) does not exhibit the inflected rise and exponential fall of its squid-axon counterpart (I_{Na}); it does exhibit similar exponential inactivation and recovery from inactivation, however. The form of the simulated potassium current (I'_K) is quite similar in all respects to its squid-axon counterpart (I_K). Quantitative comparisons are given in the text and in Figs. 23 and 24.

The circuit of Fig. 21, as it has been described in the preceding paragraphs, was designed to simulate a patch of membrane capable of spike generation. Fig. 25 shows photographs taken of oscilloscope traces of the responses of this circuit. In Fig. 25(a) a spike is shown along with the simulated sodium and potassium currents associated with it. The sodium current increases rapidly during the rising phase of the spike, then passes through a peak and begins to decline because of inactivation. The final, rapid decline of the sodium current is due to membrane repolarization on the falling phase of the spike. The peak magnitude of the simulated sodium current shown in this figure is 10 mA. This is equivalent to approximately 450 μA/cm^2 in the membrane, which is 50 percent of the value (900 μA/cm^2) calculated by Hodgkin and Huxley from their model. The simulated potassium current rises with considerable delay and, having effected repolarization, falls slowly back to its magnitude at equilibrium. The maximum potassium current in the circuit is equivalent to approximately 135 μA, which is 17 percent of the value calculated by Hodgkin and Huxley. In addition to, and compensating for, its reduced peak magnitude, the potassium current in the circuit is more prolonged than its counterpart in the Hodgkin-Huxley model. In their model, the potassium current is proportional to the product of a term that is at all times proportional to the

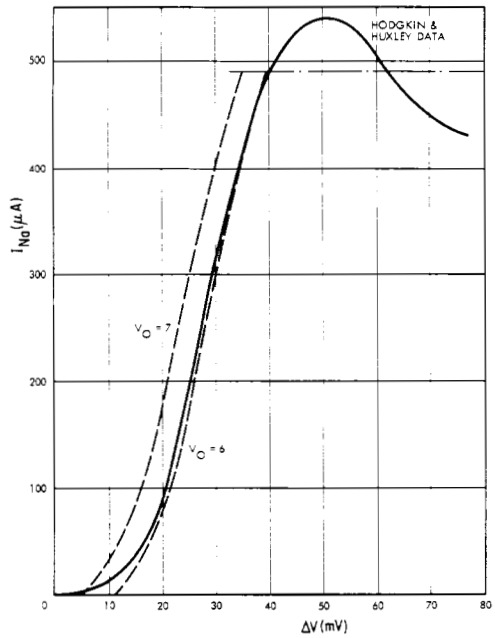

Fig. 23. Peak sodium current in response to ΔV_m, plotted against the magnitude of ΔV_m. The dashed curves are for the circuit; the solid curve is for the squid axon.[5] V_o is the voltage applied to $R11$ from variable resistor $R12$.

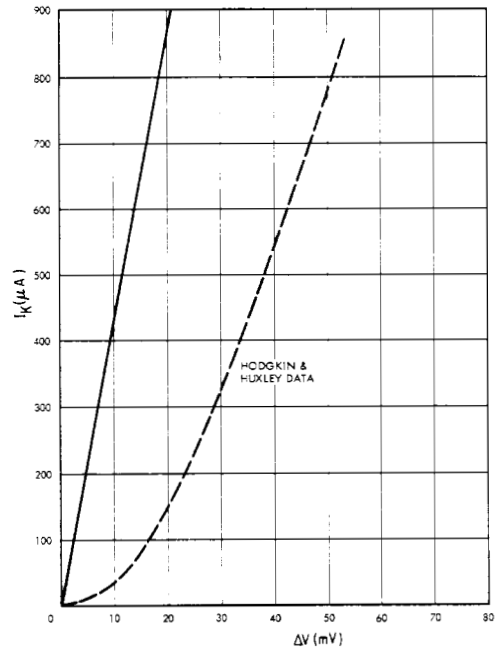

Fig. 24. Steady-state potassium current in response to ΔV_m, plotted against the magnitude of ΔV_m. The solid curve is for the circuit; the dashed curve is for the squid axon.[5]

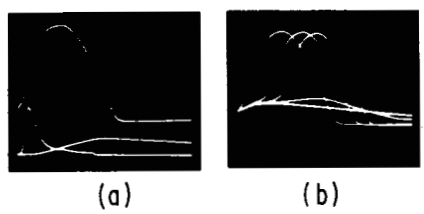

Fig. 25. Spikes from the circuit of Fig. 21. (a) Simulated membrane potential (top trace) and membrane currents (bottom traces) during spike. (b) Superimposed responses of circuit to five stimuli of different intensities.

membrane potential (the net potassium-ion driving force) and a term that tends to be proportional to the membrane potential but follows it with considerable delay (the equivalent potassium conductance). On repolarization following a spike, the net potassium-ion driving force is reduced rapidly, and the potassium current falls immediately. In the circuit, on the other hand, the product of two terms was not formed; the term with delayed dependence on membrane potential was represented, and the term with immediate dependence was omitted.

One reason for the discrepancies between peak current magnitudes in the circuit and those in the Hodgkin-Huxley model is the fact that the spike in the circuit is limited to half the equivalent amplitude of a spike in the Hodgkin-Huxley model. Apart from its reduced amplitude, the spike in Fig. 25(a) is a reasonably good replica of both the spike calculated by Hodgkin and Huxley from their model and the squid-axon spike. Each of the five successive traces in Fig. 25(b) shows the simulated internal membrane potential of the circuit after a very brief stimulus was applied to the terminal representing the inside of the membrane. The first two stimuli were very weak and elicited only subthreshold, graded responses. The third stimulus was sufficient to induce a spike, but the latency of the response was more than a millisecond. The fourth stimulus was stronger, and, although the latency was reduced considerably, the shape of the spike was essentially unchanged. The fifth stimulus was the strongest and resulted in the shortest latency.

B. A Circuit for Subthreshold Events

Over a wide range of low values of ΔV_m, the delay time of the potassium current in the Hodgkin-Huxley model is nearly constant at approximately 2 ms and the rise time is nearly constant at 10 to 12 ms. The component values listed in Table I provide delay and rise times of approximately 1 and 2 ms, respectively. While these values are appropriate for large excursions of membrane potential, such as spikes, they are not appropriate for small excursions such as postsynaptic potentials, subthreshold pacemaker potentials, and graded responses to subthreshold stimuli. In addition, while the offset voltage V_o and the nonlinear element $N1$ compensate the slope of the current-voltage relationship in the

TABLE I
COMPONENT VALUES FOR THE CIRCUIT OF FIG. 21 AS A TRIGGER REGION

*R*1	1 000 Ω	*R*24	390 Ω	*Q*1	2N1306
*R*2	3 000 Ω	*R*25	10 000 Ω	*Q*2	2N1307
*R*3	1 000 Ω	*R*26	1 000 Ω	*Q*3	2N1307
*R*4	3 000 Ω	*R*27	560 Ω	*Q*4	2N1307
*R*5	10 000 Ω	*R*28	1 000 Ω	*Q*5	2N1307
*R*6	30 000 Ω	*R*29	1 000 Ω	*Q*6	2N1306
*R*7	1 000 Ω	*R*30	2 000 Ω	*Q*7	2N1307
*R*8	1 000 Ω	*R*31	1 000 Ω	*Q*8	2N1307
*R*9	3 000 Ω	*R*32	20 000 Ω	*Q*9	2N1307
*R*10	5 100 Ω	*R*33	1 000 Ω	*Q*10	2N1306
*R*11	1 000 Ω	*R*34	7 500 Ω	*Q*11	2N1307
*R*12	10 000 Ω*	*R*35	7 500 Ω	*Q*12	2N1307
*R*13	20 000 Ω	*R*36	47 000 Ω	*Q*13	2N1307
*R*14	5 100 Ω	*R*37	2 000 Ω	*D*1	1N100
*R*15	100 000 Ω†	*R*38	1 000 Ω	*D*2	1N100
*R*16	1 000 Ω	*R*39	10 000 Ω	*D*3	1N100
*R*17	100 000 Ω	*R*40	1 000 000 Ω	*D*4	1N100
*R*18	100 Ω	*R*41	1 000 000 Ω	*N*1	023L4‡
*R*19	100 Ω	*R*42	1 000 000 Ω	*C*1	0.5 μF
*R*20	10 000 Ω†	*R*43	100 000 Ω	*C*2	0.22 μF
*R*21	2 000 Ω	*R*44	100 000 Ω	*C*3	1.0 μF
*R*22	510 Ω	*R*45	100 000 Ω	*C*4	0.22 μF
*R*23	3 900 Ω			*C*5	0.5 μF

* Potentiometer *R*12 controls the threshold for spike generation. The potential at the center tap of *R*12 should be between −6 and −7 volts (see Fig. 23).

† Variable resistor *R*20 normally should be set at 1 kΩ or less; *R*15 should be set at 20 kΩ. Increasing these resistances will introduce pronounced cumulative refractoriness in the model.

‡ Varistor.

TABLE II
COMPONENT VALUES FOR THE CIRCUIT OF FIG. 1 AS AN INTEGRATIVE REGION

*R*9	1 000 Ω
*R*13	10 000 Ω
*R*23	20 000 Ω
*R*24	2 000 Ω
*R*27	2 400 Ω
*R*28	3 900 Ω
*C*1	5 μF
*C*4	2 μF

sodium subcircuit (see Fig. 23) for small excursions of membrane potential, the slope of the current-voltage relationship of the potassium subcircuit is too steep to be applicable for small excursions. The circuit described in Section V-A represents a patch of membrane that is normally either at the resting potential or undergoing a spike and spends very little time in intermediate states. Another circuit, a simple modification of the first, can be used to represent a patch of membrane that is normally close to the resting potential and does not undergo spikes. The circuit modifications are listed in Table II. They provide the slopes and time constants appropriate for graded, nonspike activity. The new values of *R*23 and *R*24 establish the potassium delay and rise times at 2 ms and 10 ms, respectively. The new values of *R*27 and *R*28 establish the slope of the potassium current versus membrane potential at four tenths of its magnitude in Fig. 24. The new value of *C*1 provides a time constant of sodium inactivation of approximately 10 ms, while *R*13 reduces the slope of the curve of Fig. 23.

Although the modifications outlined in the preceding paragraph bring the circuit into better correspondence with the Hodgkin-Huxley model for small values of ΔV_m, one additional modification is required to eliminate the all-or-none, triggerable response (which is now a prolonged spike) and establish totally graded responses. One circuit element that can be modified to provide graded response is *C*4, the simulated transmembrane capacitance (see Lewis[111]). As the value of *C*4 is increased, the response of the circuit tends to be increasingly graded. The value of *C*4 selected for the basic modification is approximately ten times the value specified for membrane capacitance in the Hodgkin-Huxley model. Since the wires representing the inside and outside of the membrane are intended to be accessible as terminals of the circuit, the value of capacitance *C*4 can be increased further by connection of additional capacitors across these terminals.

C. Synaptic Connections

Simulated synaptic connections can be effected from a spike-generating circuit to itself, to other spike-generating circuits, and to circuits modified to yield graded response. For synaptic connection, the waveform from the sending spike-generating circuit is a negative 12-volt pulse, 2 ms in duration, taken at the output of the pulse-shaping amplifier. If this pulse is applied directly to the input terminal of a synaptic circuit, it induces a 2-ms positive- or negative-current pulse across the simulated membrane at the receiving circuit. The output voltage pulse may be applied to the synaptic circuit through a coupling filter, however, such as the one shown in Fig. 26. If the charge on *C*1 in Fig. 26 is considered analogous to a chemical synaptic transmitter, then the filter output voltage represents the transmitter concentration. The charging of *C*1 by a voltage pulse is analogous to transmitter emission, and the drain of charge through *R*2 is analogous to transmitter inactivation through a first-order process, such as simple diffusion or a first-order chemical reaction. The photographs in Fig. 27 show four examples of synaptic interactions between two circuits through the coupling filter of Fig. 26. The internal membrane potentials of the sending circuit are shown in the upper traces of each photograph. The receiving circuit had been modified according to the specifications of Table II to simulate nonspiking subsynaptic membrane. The lower trace in each photograph shows the internal membrane potential at the receiving circuit; the voltage waveforms on the lower trace have been amplified by a factor of 2 relative to the upper trace. The form of the simulated synaptic potential depends to a great extent on the values of the elements in the coupling filter. In general, the amplitude of the individual synaptic potential increases in inverse proportion to the resistance of *R*1. Rebound [Fig. 27(b)] usually occurs for small values of both *R*1 and *R*2. The prolonged inhibitory potential [Fig. 27(d)] occurs for intermediate values of *R*1 and large values of *R*2.

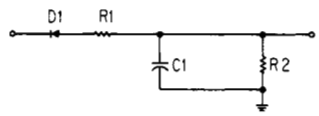

Fig. 26. Synaptic coupling circuit.

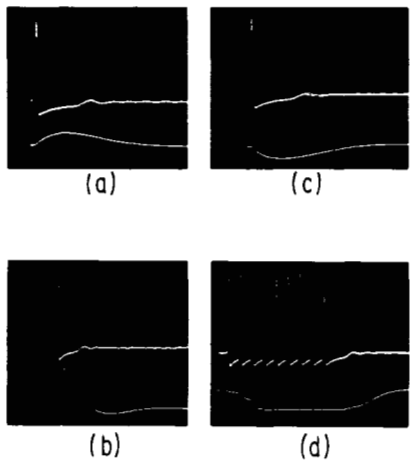

Fig. 27. Synaptic waveforms simulated by the circuit of Fig. 21. (a) An excitatory synaptic potential (lower trace) in an integrative region, elicited by a spike (upper trace) in a trigger region. (b) An excitatory postsynaptic potential with negative rebound (lower trace). (c) An inhibitory synaptic potential (lower trace). (d) Summed inhibitory potentials in response to a burst of spikes.

VI. Discussion

Because of the very nature of induction, hypotheses often are vague, general statements, not easily subjected to rigorous tests; yet a hypothesis is nearly valueless if one cannot deduce from it its necessary consequences and thus place it in jeopardy (see Platt[42]). The role of the model in biology, as I see it, is to act as the mediator between hypothesis and deduction, to be the deductively manipulable representative of the hypothesis. The transition from vague hypothesis to model implies quantification; terms must be made explicit, parameters must be identified, and causal relationships must be specified. The modern ionic hypothesis, for example, can be expressed as follows. The generation and propagation of a spike in an axon is the result of electric currents carried by specific ions passing across the axon membrane and of voltage-dependent changes in the resistance of the membrane to ion flow. In particular, the development of the spike is brought about by decreased resistance to the flow of sodium ions and a resultant influx of those ions; the recovery phase is brought about by increased resistance to the flow of sodium ions and decreased resistance to the flow of potassium ions, with a resultant efflux of the latter.

Even without quantification, this hypothesis leads to a few testable correlates. Do sodium ions tend to move into the cell during a spike? Do potassium ions tend to move out? Is the net sodium influx approximately equal to the net potassium efflux? Can a spike occur in the absence of either ion? But these are mostly qualitative questions. The Hodgkin-Huxley experiments were designed to quantify the hypothesis. They led to data explicitly relating ionic currents to membrane potential and time, but these data implied complex interactions of several variables at the axon membrane. In order to incorporate these data with the original hypothesis, Hodgkin and Huxley[5] used a mathematical model comprising ten equations. These equations were a deductively manipulable representation of the modern ionic hypothesis; deduction in this case was simultaneous solution of the equations. With their model, Hodgkin and Huxley were able to make explicit, quantitative predictions, and in doing so they placed the ionic hypothesis in jeopardy. The role of the model was to predict or deduce the necessary consequences of the hypothesis.

The electronic models discussed in this paper were intended to play the same role. They are deductively manipulable representations of a hypothesis, which can be stated as follows. A slightly modified version of the Hodgkin-Huxley description of the squid axon together with the Eccles description of a synapse provides all the essential elements of neuroelectric point processes in nerve cells. In testing the hypothesis by means of the models, one must ask a corollary question: "Does the model adequately represent the hypothesis; is the model a good realization of the Hodgkin-Huxley and Eccles descriptions?" If the answer is yes, one must then ask: "What results of the modeling study are most likely to place the hypothesis in immediate jeopardy?" Unfortunately, the second question is difficult to answer; most of the results described in this paper are qualitative and, in addition, depend on parameters that cannot be controlled with certainty in a neuron. I ask you to accept them for the present merely as speculations. The model itself is in jeopardy, however, with respect to the first question. It has predicted many explicit and testable phenomena. Consider, for example, the prediction that subthreshold oscillatory potentials whose amplitude is between 10 mV and threshold will be conducted with progressive phase lead. If this prediction proves to be incorrect, the model will be subject to redesign (see Lewis,[16] p. 75, for pertinent parameters), and the modeling studies negated, pending reexamination.

On the other hand, if the prediction proves to be correct, we must examine other predictions. Two such predictions that are rather interesting have become apparent in very recent modeling studies. Although these studies were performed with an eight-lump axon model, the predictions involve threshold rather than conduction. Both predictions apply to the squid axon at 6°C.

1) For stimuli consisting of periodic pulses, the squid axon should exhibit threshold minima at pulse intervals of approximately 32 ms and 16 ms. In addition, the stimulus pulse amplitudes required to initiate periodic spikes at these intervals should be considerably larger than the amplitudes required to sustain them (i.e., the threshold should exhibit marked hysteresis). The amplitudes required to sustain spikes at 32-ms and 16-ms intervals should be 50 to 65 percent of those required to sustain spikes at other intervals (e.g., at 13, 25, or 40 ms). For intervals shorter than 10 ms,

the threshold for initiating spikes should be high, decreasing somewhat as the interval is decreased; but the amplitude required to sustain spikes should be very low (e.g., 20 to 50 percent of that required to initiate them) and should decrease markedly with decreasing interval.

2) Following a single spike, the squid axon should exhibit at least two successive phases of hyperexcitability. The first should occur between 28 and 40 ms after the spike; the second should occur between 54 and 69 ms after the spike. Between these phases (i.e., from 40 to 54 ms after the spike), a phase of subexcitability should occur. These phases of excitability should be evident in experiments with paired, pulsatile stimuli.

Predictions 1) and 2) are both related to the same resonance phenomenon. We have alluded to this phenomenon in our discussions of oscillations and sympathetic oscillations, and it is discussed in considerable detail elsewhere.[11]

Simplifications in the Model

The electronic model used in these studies did not include most of the simplifications and approximations incorporated into the simpler model of Section V. Sodium inactivation and the immediate effect of potential on potassium current, as examples, were both incorporated as multiplicative factors.[16],[19] The most important simplifications and assumptions concerned time constants.

1) The time "constant" of recovery from sodium inactivation was taken to be *constant* at 12 ms, the only value measured by Hodgkin and Huxley.
2) The time "constant" of decline of potassium conductance in response to a negative voltage step (repolarization) was taken to be *constant* at 5 ms.
3) The time "constant" τ_n for the rise of potassium conductance in response to a positive voltage step was taken to be *constant* at 1 ms for trigger regions and at 5 ms for integrative regions. Hodgkin and Huxley had found that τ_n was voltage-dependent (see Hodgkin and Huxley,[5] p. 509).

Some consequences of varying these time constants have been examined, particularly with regard to pacemaker potentials (see Lewis,[16] pp. 102–119). The other major simplifications involved driving forces.

4) The driving force on the sodium ions was treated as a constant over almost the entire range of membrane potentials; but the simulated sodium current did approach zero as the membrane potential approached the sodium equilibrium potential.

This simplification seemed justified by the fact that during subthreshold activity, changes in sodium driving force are small compared with its total magnitude; during a spike, the membrane potential spends very little time between the subthreshold level and the sodium equilibrium potential.

5) For the same reasons, the driving force associated with the excitatory synaptic conductance was treated as a constant.

Any other differences between the model and the descriptions upon which they were based were small.

Conclusions

Although the quantitative details of the modeling results often depended critically on the quantitative details of the electronic models and the connections among them, the qualitative nature of these results often did not. The significant results of Section IV, for example, can be summarized in three speculations.

1) Mutual inhibition between a pair of spontaneously firing neurons may lead to synchrony of their spikes.
2) Mutual excitation between a pair of spontaneously firing neurons may lead to the formation of spike bursts.
3) Electrotonic connection between a pair of spontaneously firing trigger regions may be excitatory or inhibitory, depending on the phase relationships between the two regions.

These results and their obvious corollaries depend on qualitative aspects of the models, not on quantitative details. Speculation 1) is likely to prove true if the inhibitory synaptic potential rises with delay or inflection after the spike in the sending cell. Delay in synaptic response is quite common and may have several sources. Speculation 2) is likely to be true if a quenching mechanism is available. Synaptic fatigue can provide such a mechanism; so can accumulative refractoriness. Both are thought to occur in nervous systems; the latter apparently is reflected in such phenomena as Wedensky inhibition and inhibition by excessive depolarization.[43] Speculation 3) is likely to be true when spikes exhibit both positive and negative phases, a common occurrence.

The qualities that provided the phenomena of Section IV did not depend on the models being faithful realizations of the descriptions upon which they were based. The simpler models in Section V have these qualities. These simpler models have not been studied in the configurations of mutual inhibition that produced stable spike synchrony, but theoretically there seems to be little doubt that they can produce spike synchrony in mutually inhibiting pairs.[38] Wilson and Waldron[36],[44] *have* observed burst formation in mutually exciting pairs of these models, however, and also in pairs of even simpler models. Finally, both Wilson[36] and I have observed phenomena indicating that either inhibition or excitation can result from electrotonic connections between these models. So the models of Section V may be useful in some network studies, but they represent a second hypothesis, which can be stated as follows: the precise, quantitative details of neuroelectric point processes become progressively less important as one considers larger and larger neural networks. Most modelers agree, in fact, that if this hypothesis is not correct, we will face an apparently hopeless task when we set out to model the large structures of the central nervous system. I, for one, am not ready to model the human cerebellum if I must first construct 10^{10} models of point processes.

References

[1] K. S. Cole, "Dynamic electrical characteristics of the squid axon membrane," *Arch. Sci. Physiol.* (Paris), vol. 3, no. 2, pp. 253–258, 1949.

[2] A. L. Hodgkin and A. F. Huxley, "Currents carried by sodium and potassium ions through the membrane of the giant axon of *Loligo*," *J. Physiol.*, vol. 116, pp. 449–472, April 1952.

[3] ——, "The components of membrane conductance in the giant axon of *Loligo*," *J. Physiol.*, vol. 116, pp. 473–496, April 1952.

[4] ——, "The dual effect of membrane potential on sodium conductance in the giant axon of *Loligo*," *J. Physiol.*, vol. 116, pp. 497–506, April 1952.

[5] ——, "A quantitative description of membrane current and its application to conduction and excitation in nerve," *J. Physiol.*, vol. 117, pp. 500–544, August 1952.

[6] J. C. Eccles, *The Physiology of Synapses*. New York: Academic Press, 1964, pp. 49, 51, 153, 187–188.

[7] S. Hagiwara and T. H. Bullock, "Intracellular potentials in pacemaker and integrative neurons of the lobster cardiac ganglion," *J. Cell. Comp. Physiol.*, vol. 50, pp. 25–47, August 1957.

[8] T. H. Bullock, "Neuronal integrative mechanisms," in *Recent Advances in Invertebrate Physiology*, B. T. Scheer, Ed. Eugene, Ore.: University of Oregon Publications, 1957, pp. 1–20.

[9] ——, "Parameters of integrative action of the nervous system at the neuronal level," *Exptl. Cell Research Suppl.*, vol. 5, pp. 323–337, 1958.

[10] ——, "Neuron doctrine and electrophysiology," *Science*, vol. 129, pp. 997–1002, April 1959.

[11] E. R. Lewis, "Neuroelectric potentials derived from an extended version of the Hodgkin-Huxley model," *J. Theoret. Biol.*, vol. 10, pp. 125–158, January 1966.

[12] S. Hagiwara, A. Watanabe, and N. Saito, "Potential changes in syncytial neurons of lobster cardiac ganglion," *J. Neurophysiol.*, vol. 22, pp. 554–572, 1959.

[13] J. S. Coombs, J. C. Eccles, and P. Fatt, "The electrical properties of the motoneurone membrane," *J. Physiol.*, vol. 130, pp. 291–325, 1955.

[14] T. Araki and T. Otani, "The response of single motoneurones to direct stimulations," *J. Neurophysiol.*, vol. 18, pp. 472–485, 1955.

[15] L. D. Harmon and E. R. Lewis, "Neural modeling," *Physiol. Rev.*, vol. 46, pp. 513–591, July 1966.

[16] E. R. Lewis, "Models of neuroelectric interactions," Aerospace Medical Research Labs., Wright-Patterson AFB, Ohio, Rept. 67-132, 1967.

[17] E. R. Kandel and L. Tauc, "Mechanism of prolonged heterosynaptic facilitation," *Nature*, vol. 202, pp. 145–147, April 1964.

[18] P. O. Bishop, W. R. Levick, and W. O. Williams, "Statistical analysis of the dark discharge of lateral geniculate neurons," *J. Physiol.*, vol. 170, pp. 598–612, April 1964.

[19] E. R. Lewis, "An electronic model simulating neuroelectric point processes," *Kybernetik*, 1968 (in press).

[20] R. FitzHugh and H. A. Antosiewicz, "Automatic computation of nerve excitation—detailed corrections and additions," *J. Soc. Ind. Appl. Math.*, vol. 7, pp. 447–458, 1959.

[21] A. F. Huxley, "Can a nerve propagate a subthreshold disturbance," *J. Physiol.*, vol. 148, pp. 80P–81P, October 1959.

[22] J. W. Cooley and F. A. Dodge, Jr., "Digital computer solutions for excitation and propagation of the nerve impulse," *Biophys. J.*, vol. 6, pp. 583–599, September 1966.

[23] H. M. Lieberstein, "On the Hodgkin-Huxley partial differential equations," *Math. Biosciences*, vol. 1, pp. 45–69, March 1967.

[24] C. L. Prosser, D. W. Bishop, F. A. Brown, T. L. Jahn, and V. J. Wulff, *Comparative Animal Physiology*. Philadelphia: Saunders, 1950, p. 785.

[25] H. D. Crane, "Possibilities for signal processing in axon systems," in *Neural Theory and Modeling*, R. F. Reiss, Ed. Stanford, Calif.: Stanford University Press, 1964, pp. 138–153.

[26] E. R. Lewis, "The iron-wire model of nerve: a review," in *Cybernetic Problems in Bionics*, H. L. Oestreicher, Ed. New York: Gordon and Breach, 1968.

[27] D. Kennedy and D. F. Mellon, Jr., "Receptive-field organization and response patterns in neurons with spatially distributed input," in *Neural Theory and Modeling*, R. F. Reiss, Ed. Stanford, Calif.: Stanford University Press, 1964, pp. 400–413.

[28] D. M. Wilson, "The connections between the lateral giant fibers of earthworms," *Comp. Biochem. Physiol.*, vol. 3, pp. 274–284, November 1961.

[29] E. J. Furshpan and D. D. Potter, "Transmission at the giant motor synapses of the crayfish," *J. Physiol.*, vol. 145, pp. 289–325, March 1959.

[30] H. D. Crane, "Neuristor—a novel device and system concept," *Proc. IRE*, vol. 50, pp. 2048–2060, October 1962.

[31] T. H. Bullock and G. A. Horridge, *Structure and Function in the Nervous Systems of Invertebrates*. San Francisco: W. H. Freeman and Co., 1965.

[32] T. H. Bullock and C. A. Terzuolo, "Diverse forms of activity in the somata of spontaneous and integrating ganglion cells," *J. Physiol.*, vol. 138, pp. 341–364, October 1957.

[33] A. Watanabe, "The interaction of electrical activity among neurons of the lobster cardiac ganglion," *Japan J. Physiol.*, vol. 8, pp. 305–318, December 1958.

[34] R. F. Reiss, "A theory and simulation of rhythmic behavior due to reciprocal inhibition in small nerve nets," *1962 Spring Joint Computer Conf., AFIPS Proc.*, vol. 21. Palo Alto, Calif.: National Press, 1962, pp. 171–194.

[35] L. D. Harmon, "Neuromes: action of a reciprocally inhibitory pair," *Science*, vol. 146, pp. 1323–1325, December 1964.

[36] D. M. Wilson, "Central nervous mechanisms for the generation of rhythmic behavior in arthropods," *Symp. Soc. Exptl. Biol.*, vol. 20, pp. 199–228, 1966.

[37] D. H. Perkel, J. H. Schulman, T. H. Bullock, G. P. Moore, and J. P. Segundo, "Pacemaker neurons: effects of regularly spaced synaptic input," *Science*, vol. 145, pp. 61–63, July 1964.

[38] E. R. Lewis, "Neural modeling: spike synchrony as a result of mutual inhibition" (in preparation).

[39] G. D. Pappas and M. V. L. Bennett, "Specialized junctions involved in electrical transmission between neurons," *Ann. N. Y. Acad. Sci.*, vol. 137, pp. 495–508, July 1966.

[40] A. Watanabe and T. H. Bullock, "Modulation of activity of one neuron by subthreshold slow potentials in another in lobster cardiac ganglion," *J. Gen. Physiol.*, vol. 43, pp. 1030–1045, July 1960.

[41] E. R. Lewis, "Synchronization in small groups of neurons: a study with electronic models," in *Cybernetic Problems in Bionics*, H. L. Oestreicher, Ed. New York: Gordon and Breach, 1968.

[42] J. R. Platt, "Strong interference," *Science*, vol. 146, pp. 347–353, October 1964.

[43] L. Tauc, "Processus post-synaptiques d'excitation et d'inhibition dans le soma neuronique de l'aplysie et de l'escargot" (in French), *Arch. Ital. Biol.*, vol. 96, pp. 78–110, March 1958.

[44] D. M. Wilson and I. Waldron, "Models for the generation of the motor output pattern in flying locusts," this issue, page 1058.